

Noisy Image Restoration Based on Boundary Resetting BDND and Median Filtering with Smallest Window

CHENG-HSIUNG HSIEH, PO-CHIN HUANG, and SHENG-YUNG HUNG

Department of Computer Science and Information Engineering

Chaoyang University of Technology

168 Jifong E. Rd., Wufong, Taiwan 41349

E-mail: chhsieh@cyut.edu.tw

Abstract: - In this paper, a restoration approach for noisy image is proposed where a boundary resetting boundary discriminative noise detection (BRBDND) and a median filtering with smallest window (MFSW) are applied. In the proposed image restoration approach, two stages are involved: noise detection and noise replacement. The BRBDND is used to detect noisy pixels in an image. If a pixel is uncorrupted, then keep it intact. Or replace it with an uncorrupted neighborhood pixel through the MFSW. Note that miss detection happens in the BDND presented in [17] when the noise density is high. The miss detection is even worse for cases with unbalanced noisy density where the portions for the salt noise and the pepper noise are different. A boundary resetting scheme is incorporated into the BDND. By this doing, the problem of miss detection described above can be prevented. Note that a larger window used in the median filtering leads to a stronger smoothing effect on the restored image. The reported median filtering approaches, like the modified noise adaptive soft-switching median filter (MNASM) in [17], uses larger windows generally. Thus, a median filtering with smallest window (MFSW) is proposed to improve the visual quality of restored image. Two examples are provided to justify the proposed image restoration approach BRBDND/MFSW where comparisons are made with the BDND/MNASM. The results indicate that the proposed BRBDND is able to deal with the miss detection problem in the BDND. It also shows that the proposed MFSW indeed improves the visual quality of restored image as expected. The simulation results suggest that the proposed restoration approach BRBDND/MFSW generally outperforms the BDND/MNASM both in the PSNR and the visual quality of restored image.

Key-Words: - noise removal, noise detection, median filtering, BDND, image restoration

1 Introduction

Digital images are prone to be contaminated by noise which significantly degrades the visual quality or the performance of following image processing system in general. Consequently, noise removal has drawn a great deal of attention in the field of image processing. Many noisy image restoration approaches have been reported [1-3]. One of common noises is the impulse noise. During the transmission or capture process, an image may be contaminated by the impulse noise. A popular way to remove the impulse noise is the median filtering [4] or its variations [5-8]. With its simplicity, the median-based filtering schemes have been commonly used when the noise density is low. In this case, these schemes work well generally. However, for the image highly corrupted by the impulse noise the median-based approach have a difficulty to remove the impulse noise and thus an unsatisfied restored image is resulted.

To deal with the problem of median-based schemes, switching or selective schemes [9-13] for image restoration to remove impulse noise were proposed. Basically, an image restoration based on a switching scheme consists of two stages: noise detection and noise replacement. In the stage of noise detection, given a window a pixel is determined as noisy or uncorrupted. If a pixel is considered uncorrupted, then the pixel remains as it is. Otherwise, the pixel is replaced by an uncorrupted pixel within the window. Several approaches for noise detection have been reported. They can be roughly divided into three categories: fuzzy scheme as in [14-15], neural approach as in [16], and boundary-based approach as in [17]. Among the three categories, the boundary-based is preferred because of its simplicity when compared the computational complexity and system structure with the other two categories. The boundary-based approach in [17] called the boundary discriminative

noise detection (BDND) is well-known in the community of image restoration. However, as shown in [17] the BDND has difficulty to deal with cases of high noise density and unbalanced noise. In this paper we propose a boundary resetting scheme to improve the performance of BDND in those cases.

In the stage of noise replacement, many median-based schemes have been proposed. One of them was the noise adaptive soft-switching median filter (NASM) [18]. For a low and medium noise density, the NASM had a good performance. To improve the performance in cases of high noise density, a modified NASM (MNASM) was introduced in [17]. Note that the MNASM used many larger windows in the filtering process when the noise density was high. This led to a strong smoothing effect on the restored image. To improve the visual quality of restored image, a median filtering with smallest window (MFSW) is proposed in this paper where the smallest window is employed in the filtering process. By this doing, it is expected that a better restored image can be obtained.

By the proposed boundary resetting BDND (BRBDND) and the median filtering with smallest window (MFSW), an image restoration approach is presented in this paper which can be applied to an image highly contaminated by the impulse noise. This paper is organized as follows: In Section 2, the BDND in [17] is briefly reviewed where an example is provided to show the problem in the BDND. Then the proposed BRBDND is introduced in Section 3. Next the MNASM is briefly reviewed in Section 4 where an example is given to demonstrate why a larger window is used in the MNASM. In Section 5, the proposed MFSW is described. In Section 6, two examples are given to verify the proposed BRBDND and MFSW. Moreover, the performances of noise removal approaches BRBDND/MFSW and BDND/MNASM are compared in Section 6 as well. Finally, conclusion is made in Section 7.

2 Review of the BDND

In this section, the well-known noise detection approach called the BDND in [17] is reviewed. The implementation steps for the BDND are given in Section 2.1. In Section 2.2, an example is given to show the problem of miss detection in the BDND where a case of high noise density is concerned.

2.1 Implementation steps for the BDND

The BDND proposed in [17] is briefly reviewed. For details, one may consult [17]. Here, we have rephrased the steps in [17]. Given a 21×21 window,

the steps in the BDND to identify a noisy in the window are given as follows.

- Step 1. Sort pixels in the window in the ascending order and denote the resulted vector as v_o .
- Step 2. Calculate the difference of adjacent pixels in v_o and record them in vector v_d whose element is $v_d(i) = v_o(i+1) - v_o(i)$ where $v_o(i)$ are elements of v_o .
- Step 3. Find the maximum value in v_d within the indices 0 to $I_{med} = (21 \times 21 + 1) / 2$. Then the corresponding pixel in v_o is set as the lower boundary b_1 .
- Step 4. Similarly, from indices I_{med} to $(21 \times 21 - 1)$ find the maximum value in v_d and its corresponding pixel in v_o is set as the upper boundary b_2 .
- Step 5. By boundaries b_1 and b_2 , the pixel $x_{i,j}$ is clustered as the low-density cluster if $0 \leq x_{i,j} \leq b_1$, the middle cluster if $b_1 < x_{i,j} \leq b_2$, and the high-intensity cluster if $b_2 < x_{i,j} \leq 255$.
- Step 6. If the center pixel is within the middle cluster, then consider it as an uncorrupted pixel. Move the window to the next pixel and go to Step 1. Otherwise, the center pixel is noisy. Go to Step 7.
- Step 7. Resize the window to 3×3 and redo Step 1 to Step 5. Then go to Step 8.
- Step 8. If the center pixel belongs to the middle cluster, then it is considered as uncorrupted. Otherwise, the center pixel is a noisy pixel.
- Step 9. Record the detection result for all pixels in a binary matrix having same size of the image under consideration, where 1 indicates a noisy pixel and 0 otherwise.

The binary matrix obtained in Step 9 will be used in the following stage of noise replacement. It should be mentioned that there are two passes in the BDND to identify a noisy pixel. Two passes are similar except the window size for the first pass is 21×21 while 3×3 is used in the second pass. When the pixel under detection is considered as uncorrupted in the first pass, there is no need to enter into the second pass in the BDND. That is, if miss detection happens, the noisy pixel will be kept in the restored image.

2.2 An example for the BDND

Though the BDND works well in many cases, it suffers in cases of high noise density and unbalanced noise. In those cases, the number of miss detections in the BDND increases significantly. Consequently, the quality of the restored image is degraded accordingly. The reason is that in the miss detection a noisy pixel is considered as uncorrupted. The pixel remains as it is and therefore is shown in the restored image. The following example is provided to show the miss detection problem in the BDND.

A highly noisy 5×5 image block B contaminated by the salt and pepper noise is given as follows.

$$B = \begin{bmatrix} 255 & 255 & 70 & 255 & 255 & 72 & 255 \\ 255 & 0 & 255 & 71 & 255 & 0 & 255 \\ 0 & 72 & 255 & 0 & 255 & 255 & 0 \\ 255 & 0 & 81 & 255 & 0 & 0 & 255 \\ 255 & 255 & 0 & 255 & 255 & 255 & 91 \\ 0 & 255 & 255 & 0 & 82 & 0 & 255 \\ 255 & 81 & 0 & 255 & 255 & 255 & 90 \end{bmatrix}$$

By the steps described in Section 2.1, intermediate results for the example are described as follows. After Step 1, the sorted result v_o is found as

$$v_o = [0 \ 0 \ 0 \ 0 \ 0 \ 0 \ 0 \ 0 \ 0 \ 0 \ 0 \ 0 \ 0 \ 70 \ 71 \ 72 \\ 72 \ 81 \ 81 \ 82 \ 90 \ 91 \ 255 \ 255 \ 255 \ 255 \ 255 \ 255 \\ 255 \ 255 \ 255 \ 255 \ 255 \ 255 \ 255 \ 255 \ 255 \ 255 \ 255 \\ 255 \ 255 \ 255 \ 255 \ 255 \ 255 \ 255 \ 255 \ 255 \ 255]$$

By Step 2, the vector v_d is given as

$$v_d = [0 \ 0 \ 0 \ 0 \ 0 \ 0 \ 0 \ 0 \ 0 \ 0 \ 0 \ 0 \ 70 \ 1 \ 1 \ 0 \ 9 \\ 0 \ 1 \ 8 \ 1 \ 164 \ 0 \ 0 \ 0 \ 0 \ 0 \ 0 \ 0 \ 0 \ 0 \ 0 \ 0 \ 0 \ 0 \\ 0 \ 0 \ 0 \ 0 \ 0 \ 0 \ 0 \ 0 \ 0 \ 0 \ 0 \ 0 \ 0 \ 0 \ 0]$$

Then with the median index $I_{med} = (7 \times 7 + 1) / 2 = 25$, the low boundary b_1 can be found from the maximum value in $v_d(i)$ for $0 \leq i \leq I_{med}$, which is 164. The corresponding pixels in v_o are 91 and 255. Consequently, the lower boundary b_1 is set to 91. Similarly, the upper boundary b_2 is found from the maximum value in $v_d(i)$ for $I_{med} \leq i \leq 48$ which is 0. Since all pixels are 255, the upper boundary b_2 is set to 255. Thus, the ranges for the middle cluster and the high-intensity cluster are $91 < x_{i,j} \leq 255$ and $255 < x_{i,j} \leq 255$, respectively.

Note that in the given example the noisy pixel, which is of value 255, will be classified into the middle cluster and considered as an uncorrupted pixel while the high-intensity cluster is an empty set because of the inappropriate inequality. Moreover, there is no need to enter into the second pass of the BDND since the pixel under detection has been considered as uncorrupted. In other words, the noisy pixel remains as it is and therefore will be shown in the restored image. This is an undesired result in the noise removal or image restoration.

3 The Proposed BRBDNR

In this section, the motivation for the proposed noise detection scheme called the boundary resetting BDNR (BRBDND) is described and the additional steps incorporated into the BDND are introduced as well.

The reason for the miss detection happened in the example given in Section 2.2 is that the BDND has difficulty to determine the upper boundary b_2 . Similar results may happen when the lower boundary b_1 is found inappropriately. Fortunately, the problem in the determination of lower and upper boundaries can be solved by a simple but effective boundary resetting scheme.

To show how the boundary resetting scheme improves the detection performance of the BDND, the example given in Section 2.2 is reconsidered here. In the example, the miss detection can be avoided by resetting the upper boundary b_2 to b_1 . By this doing, the center pixel 255 which is noisy will be clustered into the high-intensity cluster and thus considered as a noisy pixel as it should be.

Based on the idea just described, a boundary resetting BDND (BRBDND) is proposed. In the BRBDND, two additional steps are employed in the BDNR to reset boundaries b_1 and b_2 such that the miss detection can be avoided. The two additional steps are put into Step 4 and Step 7, respectively. The modified Step 4 and Step 7 are given as follows.

Step 4. Similarly, from indices I_{med} to $(21 \times 21 - 1)$ find the maximum value in v_d and its corresponding pixel in v_o is set as the upper boundary b_2 .

Step 4a. When the maximum value in v_d within the indices 0 to I_{med} is 0, then reset $b_1 = b_2$. On the other hand, when the maximum value in v_d from indices I_{med} to $(21 \times 21 - 1)$ is 0, then reset $b_2 = b_1$.

Step 7. Resize the window to 7×7 and redo Step 1 to Step 5. Then go to Step 8.

Step 7a. When there is only one non-zero element in v_d , then reset $b_2 = b_1$.

By resetting boundaries b_1 and b_2 as in Step 4a and Step 7a, the miss detection in the BDND for the case of high noise density can be prevented. One more difference between the proposed BRBDND and the BDND in [17] is the window size in Step 7 where the former uses 7×7 and the latter 3×3 . The reason for it is that better detection performance can be achieved by our experiments.

Consider the example given in Section 2.2. It demonstrates how the boundary resetting scheme works and the miss detection is avoided. In the example, all elements of $v_d(i)$ for $I_{med} \leq i \leq 48$ are 0. Thus, by the Step 4a in the BRBDND the boundary b_2 is reset to b_1 which is 91. Therefore, the inequalities for the low-intensity cluster, the middle cluster, and the high-intensity cluster are $0 \leq x_{i,j} \leq 91$, $91 < x_{i,j} \leq 91$, and $91 < x_{i,j} \leq 255$, respectively. Therefore, the pixel under consideration is within the high-intensity cluster and identified as a noisy pixel. This avoids the miss detection in the BDND.

4 Review of the MNASM

This section gives a brief review of the noise replacement scheme called the modified NASM (MNASM) in [17]. In Section 4.1, the implementation steps are described and the problem using larger windows is mentioned. Then an example is given in Section 4.2 to show the problem of window expansion criterion in the MNASM.

4.1 Implementation steps for the MNASM

In the MNASM, the initial window size is set to 3×3 and the maximum window size to 7×7 . Denote the number of uncorrupted pixels in the current window $W_c \times W_c$ as N_c . The criterion to expand the window is $N_c < T_c = 0.5(W_c \times W_c)$. If $N_c \geq T_c$, the conventional median filtering is performed with the uncorrupted pixels in the current window when $W_c \times W_c \leq 7 \times 7$. Or the window size $W_c \times W_c$ will keep expanding until at least one uncorrupted pixel is found even the current $W_c \times W_c$ reaches the maximum window 7×7 . Once some uncorrupted pixels are found, then the conventional median filtering is used to remove the noisy pixel.

The implementation steps for the MNASM are described as follows.

Step 1. Initialize $W_c \times W_c$ as 3×3 .

Step 2. Calculate T_c and count N_c in the current window. If $N_c \geq T_c$, perform the conventional median filtering with the uncorrupted pixels in the current window and replace the noisy pixel with the median. Then move the window to the next pixel and go to Step 1. Otherwise, go to Step 3.

Step 3. If $W_c \times W_c$ does not reach to the maximum window 7×7 , then expand the window and go to Step 2. Otherwise, go to Step 4.

Step 4. Expand the $W_c \times W_c$ window till $N_c \neq 0$. Then perform the conventional median filtering.

Though the MNASM works well generally, it, however, leads to a strong smoothing effect on the restored image in the case of high noise density. By observations, the reason is that many larger windows are employed in the filtering process. The fundamental problem for this is the criterion for window expansion. In other words, the smoothing result follows the inappropriate criterion of window expansion in the MNASM. The following example given in Section 4.2 will explain the inappropriate window expansion in the MNASM.

4.2 An example for the MNASM

In this section, the problem of the window expansion in the MNASM is shown through the example given in Section 2.2. The image block B is duplicated here where different window sizes 3×3 , 5×5 , 7×7 are shown as well.

$$B = \begin{matrix} & \begin{matrix} 255 & 255 & 70 & 255 & 255 & 72 & 255 \end{matrix} \\ \begin{matrix} 255 \\ 0 \\ 255 \\ 255 \\ 0 \\ 255 \end{matrix} & \begin{matrix} \begin{matrix} 0 & 255 & 71 & 255 & 0 \end{matrix} \\ \begin{matrix} 72 & 255 & 0 & 255 & 255 & 0 \end{matrix} \\ \begin{matrix} 0 & 81 & 255 & 0 & 0 & 255 \end{matrix} \\ \begin{matrix} 0 & 255 & 255 & 0 & 82 & 0 \end{matrix} \\ \begin{matrix} 81 & 0 & 255 & 255 & 255 & 90 \end{matrix} \end{matrix} \end{matrix}$$

With the example, the filtering process of the MNASM is described as follows. In the initial window size 3×3 , there is only one uncorrupted pixel, i.e., $N_c = 1$ which is less than $T_c = 0.5(3 \times 3) = 4.5$. Thus the window is expanded to 5×5 where $N_c = 4$. Since

$N_c < T_c = 0.5(5 \times 5) = 12.5$, the window is then expanded to 7×7 where $N_c = 9$. Since $N_c < T_c = 0.5(7 \times 7) = 24.5$, thus the window is expanded further to 9×9 . By the Step 4, the MNASM will do the noise replacement in the window size 9×9 .

Note that the problem here is that T_c is increased as the window size is expanded. Though N_c increases as the window size getting larger, however it cannot catch up with T_c . This explains why the MNASM uses larger windows in the case of high noise density.

5 The Proposed MFSW

The motivation for the proposed noise replacement scheme is based on the observation in the MNASM. In the case of high noise density, the MNASM expands window size when $N_c < T_c$. However, it still generally has difficulty to find enough uncorrupted pixels within a larger window since T_c is increased as the window is expanded. Thus, a window size larger than the maximum size 7×7 is generally used in the filtering. Consequently, a restored image with strong smoothing effect is resulted. As in the example given in Section 4.2, the key problem for the MNASM is the way to expand the window. Thus a median filtering with smallest window (MFSW) is introduced in this section to improve the visual quality of restored image.

Note that the noise replacement can be achieved by substituting a noisy pixel with any uncorrupted pixel within the window. That is, the noise replacement can be done as long as, at least, one uncorrupted pixel exists in the current window. Therefore, to avoid using larger windows in the filtering process, the criterion to expand window for the proposed MFSW is that no uncorrupted pixel exists in the window. By this doing, the window will have the smallest size as it can be. Thus, the proposed noise replacement scheme is called the median filtering with smallest window (MFSW). Denote the number of uncorrupted pixels in the current window $W_c \times W_c$ as N_c . The implementation steps for the proposed MFSW are given as follows.

Step 1. Initialize $W_c \times W_c$ as 3×3 .

Step 2. Check if $N_c = 0$. If $N_c = 0$, expand the window size and redo Step 2. Otherwise, go to Step 3.

Step 3. Perform the conventional median filtering with uncorrupted pixels in the current

window and replace the noise pixel with the median.

Note that the noisy pixels have been identified in the noise detection stage. Thus the noise replacement is based on the result of noise detection. Consider the given example in Section 4.2. By the proposed MFSW, the noisy pixel will be replaced by 81 where the window size is 3×3 , instead of 9×9 as in the MNASM. Thus a better restored image can be expected in the proposed MFSW since higher correlation can be found for closer pixels generally. This will be verified in the following section.

6 Simulation Results

In this section, two examples are provided to justify the proposed BRBDND and the MFSW. Besides, the performance of the proposed noise removal or image restoration approach, the BRBDND/MFSW, will be compared with the BDND/MNASM in [17]. For fair comparison, the window size 3×3 at Step 7 for the BDND in Section 2.1 is changed to 7×7 for all related results. In the simulation, the 512×512 images Boat and Goldhill are used as examples which are contaminated by the salt and pepper noise with various noise densities. The simulation consists of three parts. In Section 6.1, the detection performance of the BRBDND is investigated under different noise densities and unbalanced noise densities. Those results are compared with those for the BDND. In Section 6.2, the replacement performance of the proposed MFSW is justified where the perfect detection is assumed. The results are compared with those from the MNASM where the application numbers of different window sizes in the MFSW and the MNASM are compared. In Section 6.3, the restored images from the BRBDND/MFSW are evaluated and compared with the BDND/MNASM in terms of peak signal-to-noise ratio (PSNR) and subjective visual assessments.

6.1 Detection Performance of the BRBDND

To evaluate the detection performance, images Boat and Goldhill are first contaminated by the balanced salt and pepper noise (BSPN) and the unbalanced SPN (USPN), varied from 10% to 90%. The balanced BSPN means the salt noise and pepper noise are equally distributed in the images while the USPN has different portions of salt and pepper noise. For example, the 80%+10% USPN means the total noise density is 90% where 80% is the pepper noise

and 10% the salt noise. Then the detection results of the BRBDND and the BDND for the BSPN and USPN are obtained.

(A) BSPN

For the BSPN, the detection results of the proposed BRBDND for images Boat and Goldhill are, respectively, recorded in Table 1 and Table 2 where MD stands for the miss detection and FA the false alarm. The miss detection considers a noisy pixel as an uncorrupted one and the false alarm considers an uncorrupted pixel as a noisy one. The MD affects the restored image much more than that in the FA since the noisy pixel remains in the restored image while the FA replaces an uncorrupted pixel with another uncorrupted one in the noise replacement stage.

For comparison, the corresponding results obtained from the BDND are shown in Table 1 and Table 2 as well. Table 1 and Table 2 indicate that the BRBDND has zero MD for all cases while the BDND has few MD in the case with 80% noise density and over two thousand for the 90% case. As for the FA, both BRBDND and BDND have identical performance except the 90% case. By the results, it indicates that the proposed BRBDND is able to deal with the miss detection problem while the BDND fails to. In other words, the BRBDND improves the detection performance of the BDND.

Table 1 Detection performance of the BSPN for the BRBDND and the BDND (Boat)

Noise density	MD		FA	
	BRBDND	BDND	BRBDND	BDND
10%	0	0	296	296
20%	0	0	326	326
30%	0	0	200	200
40%	0	0	302	302
50%	0	0	231	231
60%	0	0	283	283
70%	0	0	187	187
80%	0	1	218	218
90%	0	2,916	201	192

Table 2 Detection performance of the BSPN for the BRBDND and the BDND (Goldhill)

Noise density	MD		FA	
	BRBDND	BDND	BRBDND	BDND
10%	0	0	30	30
20%	0	0	30	30
30%	0	0	27	27
40%	0	0	30	30
50%	0	0	21	21
60%	0	0	25	25
70%	0	0	18	18
80%	0	3	11	11
90%	0	2,546	49	40

(B) USPN

The results obtained from the proposed BRBDND and the BDND for the USPN are given in Tables 3 and 4, respectively, for images Boat and Goldhill. Again, the BRBDND has zero MD for all cases. However, the BDND is not able to handle the cases with USPN. As for the FA, the proposed BRBDND always is a little higher than the BDND. However, it does not affect the restored image too much since the amount of FA is not high. It seems that the BRBDND trades a little FA for zero MD.

Table 3 Detection performance of the USPN for the BRBDND and the BDND (Boat)

Noise density	MD		FA	
	BRBDND	BDND	BRBDND	BDND
80%+10%	0	186	1,286	434
70%+20%	0	320	1,227	421
60%+30%	0	480	1,320	442
50%+40%	0	679	623	301
40%+50%	0	70,090	819	606
30%+60%	0	157,375	1,269	830
20%+70%	0	182,328	1,346	880
10%+80%	0	209,394	1,213	781

Table 4 Detection performance of the USPN for the BRBDND and the BDND (Goldhill)

Noise density	MD		FA	
	BRBDND	BDND	BRBDND	BDND
80%+10%	0	177	398	118
70%+20%	0	344	368	90
60%+30%	0	559	421	136
50%+40%	0	717	170	63
40%+50%	0	69,085	219	166
30%+60%	0	157,160	349	251
20%+70%	0	182,309	395	285
10%+80%	0	209,142	430	290

6.2 Replacement Performance of the MFSW

In this section, the performance of the proposed MFSW is justified. For a fair comparison with the MNASM, the perfect detection is assumed in the following simulation, i.e., no MD and no FA happens. Only the BSPN is under consideration here. Two comparisons are made: the PSNR and the application numbers of different window sizes in the filtering process.

(A) PSNR

The PSNR obtained from the proposed MFSW and the MNASM for images Boat and Goldhill are shown in Figure 1. For both images, the proposed MFSW and the MNASM have similar PSNR in lower noisy densities. For other cases, the proposed MFSW has better PSNR than the MNASM.

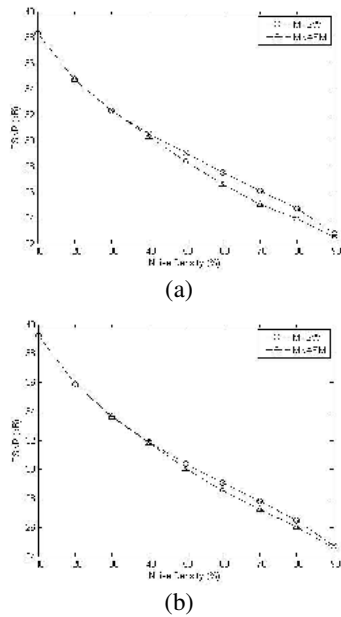


Fig. 1 The PSNR for the MFSW and the MNASM (a) Boat (b) Goldhill

(B) The application numbers of window sizes

The application numbers of different window sizes in the filtering process are investigated both for the MFSW and the MNASM. Since similar results are found in both images, only image Boat is under consideration. The application numbers of different window sizes in the MFSW and the MNASM are given in Tables 5 and 6, respectively. The results show that the application numbers of different window sizes are mostly distributed among smaller windows for the proposed MFSW. However, the distribution for the MNASM generally is among larger windows, especially for cases with higher noise densities.

Table 5 The application numbers of window sizes in the MFSW (Goldhill)

Window size	3×3	5×5	7×7	9×9 and up
10%	26,213			
20%	52,437			
30%	78,701	5		
40%	105,135	85		
50%	130,511	481		
60%	154,398	2,693	1	
70%	172,887	10,326	30	
80%	174,806	33,876	945	4
90%	134,572	83,201	16,681	1,389

Table 6 The application numbers of window sizes in the MNASM (Goldhill)

Window size	3×3	5×5	7×7	9×9 and up
10%	26,201	12		
20%	51,932	501	4	
30%	74,115	4,111	453	27
40%	86,634	11,996	4,209	2,381
50%	83,735	15,185	7,586	24,486
60%	64,104	8,453	2,445	82,090
70%	35,574	1,675	98	145,896
80%	11,703	60	0	197,868
90%	1,218	0	0	234,625

To see how the window size affects the visual quality, the Boat shown in Figures 2 and 3 are restored from the cases of 30% and 80% noise density, respectively. Both restored images from the 30% noise density for the proposed MFSW and the MNASM have similar visual quality since the window size 3×3 used in the filtering process most of time as indicated in Tables 5 and 6. As for the case of 80% noise density, the proposed MFSW usually applies 3×3 window in the filtering while the MNASM mostly uses window size 9×9 and up. As shown in Figure 3, a stronger smoothing effect is found in the restored image for the MNASM while the MFSW retains more details in the restore Boat. The results shown in Figures 2 and 3 suggest that the window size used in the filtering process has smoothing effect on the restored image. That is, a larger window leads to a stronger smoothing effect and vice versa.



Fig. 2 Restored Goldhill by (a) the MNASM (b) the MFSW (30% BSPN)



Fig. 3 Restored Goldhill by (a) the MNASM (b) the MFSW (80% BSPN)

6.3 Performance of the BRBDND/MFSW

In this section, the proposed BRBDND and MFSW are integrated into a noise removal approach called the BRBDND/MFSW, which is applied to noisy image restoration. Both the BSPN and the USPN are considered in the simulation. Moreover, the results of the proposed BRBDND/MFSW are compared with those for the BDND/MNASM.

(A) BSPN

The PSNR for the restored Boat and Goldhill with the BSPN are given in Figure 4 where the corresponding PSNR from the BDND/MNASM are also shown. From Figure 4, it indicates the BRBDND/MFSW generally has better PSNR than the BDND/MNASM, especially for the 90% case. It is because the BDND has a large amount of MD in the 90% case as shown in Tables 1 and 2. Therefore, many noisy pixels remain in the restored image.

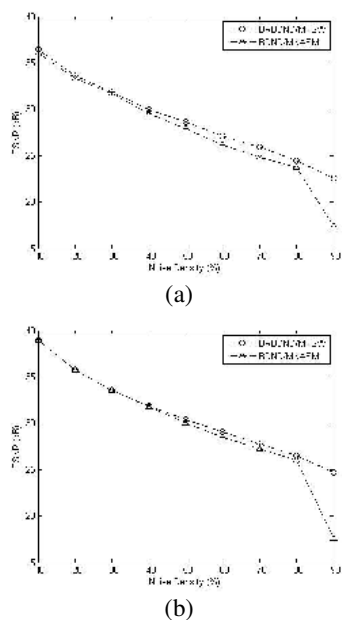


Fig. 4 The PSNR for the BSPN with BRBDND/MFSW and the BDND/MNASM (a) Boat (b) Goldhill

As for the visual quality, the restored Boat and Goldhill from 80% noise density by the BRBDND/MFSW and the BDND/MNASM are shown in Figures 5 and 6, respectively. As expected, the restored images from the BRBDND/MFSW have better visual quality because better replacement performance is achieved in the MFSW. The restored Boat and Goldhill by the BDND/MNASM show a strong smoothing effect because many larger windows are employed in the median filtering. On the other hand, the proposed

MFSW uses the smallest window possible in the filtering process and thus has better visual quality with more details.

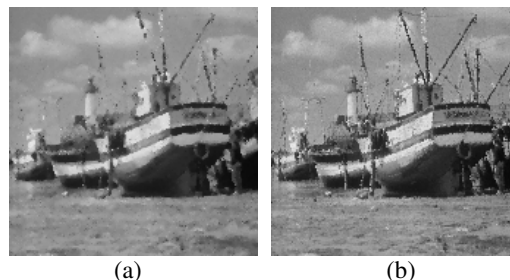


Fig. 5 Restored Boat by (a) the BDND/MNASM (b) the BRBDND/MFSW (80% BSPN)



Fig. 6 Restored Goldhill by (a) the BDND/MNASM (b) the BRBDND/MFSW (80% BSPN)

(B) USPN

As for the USPN, the PSNR for the proposed BRBDND/MFSW and the BDND/MNASM are given in Tables 7 and 8. The results indicate that the BRBDND/MFSW has better PSNR than the BDND/MNASM for the first four cases while having much better PSNR for the other cases. It should be noted that the proposed BRBDND/MFSW obtains similar PSNR for all cases. It suggests that the BRBDND/MFSW is able to handle the USPN very well. However, the BDND has a problem in the detection of the USPN, especially for cases with large portions of the salt noise. By the detection results shown in Tables 3 and 4, the number of MD is increased significantly as the portions of the salt noise is increased. It means that many pixels contaminated by the salt noise remain in the restored images. Even in a better case, say the 80%+10% case, the BDND/MNASM still has difficulty to deal with the salt noise as shown in Figures 7 and 8 where while pixels are the remained noisy pixels corrupted by the salt noise.

In summary, the proposed noise removal approach BRBDND/MFSW generally has better performance than the BDND/MNASM in [17] both in the PSNR and the visual quality of restored

images, where both the BSPN and USPN are considered.

Table 7 The PSNR for the USPN with BRBDND/MFSW and the BDND/MNASM (Boat)

Noise density	PSNR	
	BRBDND/MFSW	BDND/MNASM
80%+10%	21.87	21.64
70%+20%	21.79	21.48
60%+30%	21.79	20.96
50%+40%	22.32	20.71
40%+50%	22.32	7.66
30%+60%	21.85	6.06
20%+70%	21.85	6.03
10%+80%	21.88	6.02

Table 8 The PSNR for the USPN with BRBDND/MFSW and the BDND/MNASM (Goldhill)

Noise density	PSNR	
	BRBDND/MFSW	BDND/MNASM
80%+10%	24.43	23.96
70%+20%	24.46	22.47
60%+30%	24.31	22.18
50%+40%	24.57	20.97
40%+50%	24.66	6.64
30%+60%	24.53	5.03
20%+70%	24.43	5.01
10%+80%	24.45	5.00

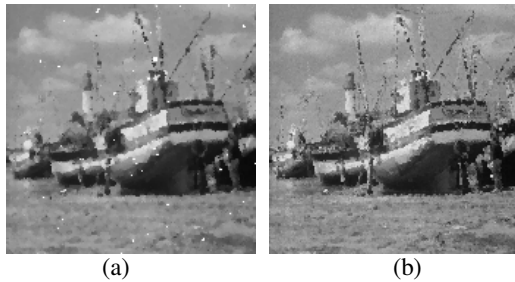


Fig. 7 Restored Boat by (a) the BDND/MNASM (b) the BRBDND/MFSW (80%+10% USPN)



Fig. 8 Restored Goldhill by (a) the BDND/MNASM (b) the BRBDND/MFSW (80%+10% USPN)

7 Conclusion

A noisy image restoration approach applied to an image highly contaminated by the SPN has been presented in this paper. Two stages are involved: noise detection and noise replacement. In this paper, the boundary resetting BDND (BRBDND) for noise detection has been introduced. By resetting boundaries in the BDND, the detection performance of the BDND has been improved significantly and is able to deal with cases of high noise density and unbalanced noise. For the noise replacement, the median filtering with smallest window (MFSW) has been proposed. In the MFSW, the criterion to expand window is no uncorrupted pixel exists in the current window. By this doing, the smallest window used in the median filtering is guaranteed and a restored image of better visual quality has been obtained when compared with the MNASM in [17]. Simulation results have justified the feasibility of the proposed approach BRBDND/MFSW and have indicated the BRBDND/MFSW is better than the BDND/MNASM in [17] both in the PSNR and the visual quality of restored images.

Acknowledgement

This work was supported by the National Science Council of the Republic of China under grant NSC 97-2221-E-324-032.

References:

- [1] P. Bojarczak and S. Osowski, "Denoising of Images - A Comparison of Different Filtering Approaches," *WSEAS Transactions on Computers*, Issue 3, Vol.3, pp.738-743, July 2004.
- [2] A. Khare and U. S. Tiwary, "Symmetric Daubechies Complex Wavelet Transform and Its Application to Denoising and Deblurring," *WSEAS Transactions on Signal Processing*, Issue 5, Vol.2, pp.738-745, May 2006.
- [3] H. Furuya, S. Eda, and T. Shimamura, "Image Restoration via Wiener Filtering in the Frequency Domain," *WSEAS Transactions on Signal Processing*, Issue 2, Vol.5, pp.63-73, February 2009.
- [4] I. Pitas and A. N. Venetsanopoulos, "Order Statistics in Digital Image Processing," *Proceedings of the IEEE*, Vol. 80, No. 12, pp. 1893-1921, December 1992.
- [5] D. R. K. Brownrigg, "The Weighted Median Filter," *Communications of the ACM*, Vol. 27, No. 8, pp. 807-818, August 1984.

- [6] S.-J. Ko and Y. H. Lee, "Center Weighted Median Filters and Their Applications to Image Enhancement," *IEEE Transactions on Circuits and Systems*, Vol. 38, No. 9, pp. 984-993, September 1991.
- [7] A. Nieminen, P. Heinonen and Y. Neuvo, "A New Class of Detail-Preserving Filters for Image Processing," *IEEE Transactions on Pattern Analysis and Machine Intelligence*, Vol. 9, No. 1, pp. 74-90, January 1987.
- [8] G. R. Arce and R. E. Foster, "Detail-Preserving Ranked-Order based Filters for Image Processing," *IEEE Transactions on Acoustics, Speech, and Signal Processing*, Vol. 37, No. 1, pp. 83-98, January 1989.
- [9] T. Chen, K.-K. Ma, and L.-H. Chen, "Tri-State Median Filter for Image Denoising," *IEEE Transactions on Image Processing*, Vol. 8, No. 12, pp. 1834-1838, December 1999.
- [10] S. Zhang and M. A. Karim, "A New Impulse Detector for Switching Median Filters," *IEEE Signal Processing Letters*, Vol. 9, No. 4, pp. 360-363, November 2002.
- [11] G. Pok, J.-C. Liu, and A. S. Nair, "Selective Removal of Impulse Noise Based on Homogeneity Level Information," *IEEE Transactions on Image Processing*, Vol. 12, No. 1, pp. 85-92, January 2003.
- [12] U. Ghanekar, A. K. Singh and R. Pandey, "A New Scheme for Impulse Detection in Switching Median Filters for Image Filtering," *International Conference on Conference on Computational Intelligence and Multimedia Applications*, Vol. 3, 13-15, pp. 442-446, December 2007.
- [13] P. Wei, J. Li, D. Lu, and G. Chen, "A Fast and Reliable Switching Median Filter for Highly Corrupted Images by Impulse Noise," *IEEE International Symposium on Circuits and Systems*, pp. 3427-3430, May 2007.
- [14] S. Schulte, M. Nachtgael, V. D. Witte, D. V. Weken, and E. E. Kerre, "A Fuzzy Impulse Noise Detection and Reduction Method," *IEEE Transactions on Image Processing*, Vol. 15, No. 5, pp. 1153-1162, May 2006.
- [15] S. Schulte, V. D. Witte, M. Nachtgael, D. V. Weken, and E. E. Kerre, "Fuzzy Two-Step Filter for Impulse Noise Reduction From Color Images," *IEEE Transactions on Image Processing*, Vol. 15, No. 11, pp. 3567-3578, November 2006.
- [16] Y.-T. Zhou, R. Chellappa, A. Vaid, and B. K. Jenkins, "Image Restoration Using a Neural Network," *IEEE Transactions on Acoustics, Speech, and Signal Processing*, Vol. 36, No. 7, pp. 1141-1151, July 1989.
- [17] P.-E. Ng and K.-K. Ma, "A Switching Median Filter With Boundary Discriminative Noise Detection for Extremely Corrupted Images," *IEEE Transactions on Image Processing*, Vol. 15, No. 6, pp. 1506-1516, June 2006.
- [18] H.-L. Eng and K.-K. Ma, "Noise Adaptive Soft-switching Median Filter," *IEEE Transactions on Image Processing*, Vol. 10, No. 2, pp. 242-251, February 2001.